Published in final edited form as:
J Exp Bot. 2023 January 18; 74(6): 1940–1956. doi:10.1093/jxb/erad020.

The transcription factor AtMYB12 is part of a feedback loop regulating cell division orientation in the root meristem vasculature

Brecht Wybouw[#1,2], **Helena E. Arents**[#1,2], **Baojun Yang**[1,2], **Jonah Nolf**[1,2], **Wouter Smet**[1,2,3], **Michael Vandorpe**[1,2], **Max Minne**[1,2], **Xiaopeng Luo**[1,2], **Inge De Clercq**[1,2], **Daniël Van Damme**[1,2], **Matouš Glanc**[1,2,#], **Bert De Rybel**[1,2,#,†]

Brecht Wybouw: brechtwybouw@helsmki.fi; Helena E. Arents: helena.arents@gmail.com; Baojun Yang: bayan@psb.vib-ugent.be; Jonah Nolf: jonol@psb.vib-ugent.be; Wouter Smet: wouter.smet@kaust.edu.sa; Michael Vandorpe: midor@psb.vib-ugent.be; Max Minne: max.minne@psb.vib-ugent.be; Xiaopeng Luo: xiaopeng.luo@psb.vib-ugent.be; Inge De Clercq: inge.declercq@psb.vib-ugent.be; Daniël Van Damme: dadam@psb.vib-ugent.be; Matouš Glanc: magla@psb.vib-ugent.be

[1]Ghent University, Department of Plant Biotechnology and Bioinformatics, Technologiepark 71, 9052 Ghent, Belgium

[2]VIB Center for Plant Systems Biology, Technologiepark 71, 9052 Ghent, Belgium

[#] These authors contributed equally to this work.

Abstract

Transcriptional networks are crucial to integrate various internal and external signals into optimal responses during plant growth and development. Primary root vasculature patterning and proliferation are controlled by a network centred around the basic Helix-Loop-Helix transcription factor complex formed by TARGET OF MONOPTEROS 5 (TMO5) and LONESOME HIGHWAY (LHW), which control cell proliferation and division orientation by modulating cytokinin response and other downstream factors. Despite recent progress, many aspects of the TMO5/LHW pathway are not fully understood. In particular, the upstream regulators of TMO5/LHW activity remain unknown. Here, using a forward genetic approach to identify new factors of the TMO5/LHW pathway, we discovered a novel function of the MYB-type transcription factor MYB12. MYB12 physically interacts with TMO5 and dampens the TMO5/LHW-mediated induction of direct target gene expression as well as the periclinal/radial cell divisions. The expression of *MYB12* is activated by the cytokinin response, downstream of TMO5/LHW, resulting in a novel MYB12-mediated negative feedback loop that restricts TMO5/LHW activity to ensure optimal cell proliferation rates during root vascular development.

[†] Corresponding author bert.derybel@psb.vib-ugent.be (B.D.R.).
[#]Co-senior authors
[3]current address: King Abdullah University of Science and Technology, Division of Biological and Environmental Sciences and Engineering, Thuwal 23955-6900, Saudi Arabia

Author Contributions:
B.D.R. conceived the project; B.D.R., M.G., D.V.D., B.W. and H.E.A. designed experiments and analysed data; B.W., H.E.A., B.Y., J.N., W.S., M.V. and M.G. performed experiments; ; M.M., X.L. and I.D.C. contributed to revising the manuscript; B.D.R. and M.G. supervised the project and wrote the paper with input of all authors.

Conflict of interest:
The authors declare no conflict of interest.

Europe PMC Funders Author Manuscripts

Keywords

Arabidopsis thaliana; cytokinin; EMS screen; root development; transcription factors; vascular development

Europe PMC Funders Author Manuscripts

Introduction

Transcription factors (TFs) play a crucial role in controlling virtually all developmental processes in eukaryotes by regulating the expression of specific subsets of target genes. TFs do not typically act alone but are embedded in complex transcriptional networks, which modulate their activity to ensure optimal transcriptional output in response to various environmental and developmental signals. Transcriptional networks often rely on feedback regulation, where a TF promotes the expression of its own activator (positive feedback) or repressor (negative feedback), respectively (Ohashi-Ito and Fukuda, 2020).

During vascular development in the plant embryo and primary root apical meristem, the heterodimer complex formed by the basic Helix-Loop-Helix (bHLH) TFs TARGET OF MONOPTEROS 5 (TMO5) and LONESOME HIGHWAY (LHW) controls vascular cell proliferation leading to radial expansion of the vascular bundle (De Rybel *et al.*, 2014; De Rybel *et al.*, 2013; Ohashi-Ito and Bergmann, 2007; Ohashi-Ito *et al.*, 2013; Ohashi-Ito *et al.*, 2014). The TMO5/LHW dimer is active in xylem cells, where it directly activates the expression of *LONELY GUY 3* (*LOG3*), *LOG4* and *BETA GLUCOSIDASE 44* (*BGLU44*), encoding key enzymes in the biosynthesis and deconjugation of cytokinin (De Rybel *et al.*, 2014; Kurakawa *et al.*, 2007; Kuroha *et al.*, 2009; Ohashi-Ito *et al.*, 2014; Yang *et al.*, 2021). This leads to a local increase of cytokinin, which is thought to diffuse to the neighbouring procambium cells (De Rybel *et al.*, 2014; Ohashi-Ito *et al.*, 2014) and trigger the expression of members of the DNA-BINDING WITH ONE FINGER (DOF) type TF family (Miyashima *et al.*, 2019; Smet *et al.*, 2019). These DOF-type TFs in turn lead to a switch in division plane orientation from anticlinal to periclinal and radial in specific subsets of procambium and phloem pole cells, depending on the DOF family member. The actual molecular mechanisms are however not yet fully explored (Otero *et al.*, 2022). The activity of the TMO5/LHW complex is negatively regulated by members of the SUPPRESSOR OF ACAULIS51-LIKE (SACL) subclade of bHLH TFs (Katayama *et al.*, 2015; Vera-Sirera *et al.*, 2015). Similarly to TMO5, SACLs physically interact with LHW. By competing with TMO5 for LHW binding, the SACLs reduce the amount of functional TMO5/LHW complexes, and thus dampen the activity of the pathway (Katayama *et al.*, 2015; Vera-Sirera *et al.*, 2015). As *SACL* genes are themselves downstream targets of TMO5/LHW, they constitute a typical negative feedback loop (Katayama *et al.*, 2015; Vera-Sirera *et al.*, 2015).

Besides forming bHLH homo- or heterodimers, bHLH proteins have also been shown to directly interact with other proteins such as MYB-type TFs, which can enhance or supress their transcriptional activity (Carretero-Paulet *et al.*, 2010; Cui *et al.*, 2021; Feller *et al.*, 2011; Zhao *et al.*, 2008). MYB TFs are defined by their highly conserved DNA-binding MYB-domain that contains up to four α-helical “R” repeats (Du *et al.*, 2009; Ogata *et al.*, 1996). The class (R1, R2 or R3, depending on their similarity to c-Myb R repeats)

and number of the R repeats are the basis of MYB protein classification (Dubos *et al.*, 2010). Most plant MYBs belong to the R2R3-MYB subfamily (Stracke *et al.*, 2001), which is involved in a plethora of processes including phenylpropanoid biosynthesis (Liu *et al.*, 2015), development of tissues and organs (Lee and Schiefelbein, 1999; Oppenheimer *et al.*, 1991) and hormonal responses (Jin and Martin, 1999). Exemplary bHLH-MYB interactions take place during epidermal cell fate specification. The formation of trichomes and root hairs depends on the assembly of different heterotrimeric bHLH/WD40/MYB complexes. In addition to the WD40 protein TRANSPARENT TESTA GLABRA 1 (TTG1), the core bHLH proteins GLABRA 3 (GL3) or ENHANCER OF GLABRA 3 (EGL3) interact with the R2R3 MYB proteins WEREWOLF (WER) or GLABRA 1 (GL1), forming an active transcriptional complex that promotes root hair or trichome formation, respectively. Alternatively, the recruitment of CAPRICE (CPC), TRIPTYCHON (TRY) or ENHANCER OF TRY AND CPC 1, single-repeat R3 MYBs that lack the C-terminal transcriptional activation domain and compete with the active R2R3 MYBs for bHLH binding, results in the formation of a transcriptionally inactive complex that prevents trichome/root hair formation (Kirik *et al.*, 2004; Ramsay and Glover, 2005; Tominaga-Wada *et al.*, 2017; Wada *et al.*, 1997). The single-repeat R3 MYBs are downstream targets of the active MYB/bHLH/WD40 complex, and at the same time its non-cell autonomous inhibitors. The bHLH and MYB TFs thus constitute a negative feedback loop that lies at the core of epidermal cell type specification and patterning (Song *et al.*, 2015; Wang *et al.*, 2008). A similar bHLH/MYB/WD40 complex controls the expression of a core enzyme in the proanthocyanin biosynthetic pathway (Appelhagen *et al.*, 2011; Xu *et al.*, 2015; Xu *et al.*, 2013). As such, interactions between MYB and bHLH TFs are key to various developmental processes.

The closely related R2R3 MYB proteins MYB11, MYB12 and MYB111 promote the expression of genes encoding key flavonol biosynthetic enzymes (Mehrtens *et al.*, 2005; Stracke *et al.*, 2007; Stracke *et al.*, 2010; Stracke *et al.*, 2017). Flavonols are a subgroup of flavonoids, besides the red to purple anthocyanins and brown proanthocyanidins (Lepiniec *et al.*, 2006; Winkel-Shirley, 2001). Flavonoids convey color to fruits and seeds and aid in abiotic stress response (Wang *et al.*, 2016). MYB11, MYB12 and MYB111 induce flavonol biosynthesis at different developmental stages, depending on their distinct expression patterns: While MYB12 is mostly active in roots, MYB11 acts in meristematic tissues and MYB111 functions in the hypocotyl and cotyledons (Stracke *et al.*, 2007). The genes encoding flavonol biosynthesis enzymes *CHALCONE SYNTHASE* (*CHS*), *CHALCONE FLAVANONE ISOMERASE* (*CHI*), *FLAVANONE 3'-HYDROXYLASE* (*F3'H*), and *FLAVONOL SYNTHASE* (*FLS*) catalyse consecutive steps of flavonol production (Forkmann and Martens, 2001) and are regulated by MYB TFs via the MYB recognition element in their promoter regions. *CHS* and *FLS* are directly transcriptionally activated by MYB12 (Mehrtens *et al.*, 2005). Consequently, the levels of the flavonols kaempferol and quercetin are decreased in the *myb12* mutant, while *MYB12* overexpression leads to increased flavonol levels (Mehrtens *et al.*, 2005).

Here, we discover a novel role of MYB12 as a negative regulator of the TMO5/LHW pathway during vascular proliferation. *MYB12* is a downstream target of TMO5/LHW; interacts with TMO5 and represses TMO5/LHW transcriptional activity, thus constituting a negative feedback loop in the regulation of vascular development. Our work highlights

Europe PMC Funders Author Manuscripts

the importance of bHLH-MYB interactions in multiple developmental processes; and demonstrates concomitant activator and repressor functions of the same TF in different transcriptional network contexts.

Materials and Methods

Plant material and growth conditions

Seedlings were grown at 22°C under continuous light on ½ Murashige and Skoog (MS) medium without 1% sucrose, after seeds were stratified for 24h-48h. For dexamethasone (DEX) treatment, 10 μM DEX (Sigma-Aldrich) was added to the growth medium from a 10 mM DMSO stock solution; seedlings were either germinated on DEX-containing medium or transferred from MS medium at the indicated time point. For the CK sensitivity assay, seedlings were germinated on 10μM 6-benzylaminopurine (6-BAP; Duchefa)-containing medium. For the CK treatment of p*MYB12*::nGFP/GUS, 5-day old seedlings were incubated in liquid ½ MS supplemented with 10μM 6-BAP for 6h.The AGI identifiers for the genes used in this manuscript are as followed: *TMO5 (AT3G25710), LHW (AT2G27230), MYB11* (*AT3G62610*), *MYB12* (*AT2G47460*), *MYB111* (*AT5G49330*), *LOG4* (*AT3G53450*), *GH10* (*AT4G38650*) and *ARR5* (*AT3G48100*). The following mutant and transgenic lines were described previously: *myb12-1f* (Mehrtens et al., 2005)*; myb11 myb12-1f myb111* (*myb* triple) (Stracke *et al.*, 2007); p*RPS5A*::TMO5:GR x p*RPS5A*::LHW:GR (dGR) (Smet *et al.*, 2019); p*LOG4*::n3GFP; p*TMO5*::nGFP/GUS (De Rybel *et al.*, 2014). The lines *ins4/lhw-8* and *hyp2/myb12-2* were generated in the dGR background by EMS mutagenesis (see below). The lines p*GH10*::n3GFP, p*RPS5A*::MYB12, p*RPS5A*::MYB12 *hyp2*, p*MYB12*::nGFP-GUS and p*MYB12*::gMYB12:sYFP were obtained by transforming the respective expression clones into Col-0 or *hyp2* by the floral dip method (Clough and Bent, 1998). The p*LOG4*::n3GFP and p*GH10*::n3GFP were introduced into the dGR and p*RPS5A*::MYB12 *hyp2/myb12-2* dGR backgrounds by genetic crossing and analysed in F1 generation seedlings.

EMS mutagenesis and screening

The dGR line (Smet *et al.*, 2019) was used for the EMS mutagenesis. Approximately 10,000 seeds were incubated shaking in water overnight. The water was replaced with 15 ml of 0.05 % Triton X-100. After mixing well, the seeds were incubated for 5 min in this solution then twice washed with water. The seeds were mutagenized by treatment with 30 mM EMS in 0.1 M phosphate buffer (pH 7.5) for 6-7 hours. Afterwards, the EMS solution was removed, and mutagenesis was stopped by adding 0.1 M $Na_2S_2O_3$ for 5 min five times. The $Na_2S_2O_3$ was washed away with water seven times. These seeds were afterwards stratified in 0.1% agarose overnight. Approximately 50 seeds were sown together in a pot per pool. A total of 228 pools was maintained. For each pool, about 1,000 M_2 seeds were initially screened on 10 μM DEX containing ½ MS media, leading to a selection of 260 mutants from 110 pools. Next, the root length and root width of one-week-old M_3 seedlings was measured in both mock (DMSO) and 10 μM DEX. Changes in root length and meristem width were measured upon DEX treatment and compared to a Col-0 and dGR control.

Mapping causal mutation of EMS mutants

Selected EMS mutants were backcrossed with the parental dGR line, and one-week-old BC_1F_2 seedlings with the desired phenotype were collected for DNA extraction. DNA was extracted using hexadecyltrimethylammoniumbromide (CTAB) extraction buffer (0.1 M Tris pH7.5, 0.7M NaCl, 0.01 M EDTA and 0.03 M CTAB) and afterwards isolated using chloroform:isoamylalcohol (24:1) and isopropanol. RNA was degraded by RNase treatment between the chloroform and isopropanol isolation steps. The bulked genomic DNA was sequenced by using the Illumina NextSeq 500 system. For the library preparation, an insert size of 400-500 bp was used. Paired end sequencing was performed, with a read length of 2x150 bp length and 50x coverage. Potential causal mutations were selected using the SHORE map analysis tool (Schneeberger *et al.*, 2009).

Molecular cloning

The promoters and coding sequences were PCR-amplified using a high-fidelity polymerase (primers used are shown in Table S3). All constructs were made by MultiSite Gateway cloning (Karimi *et al.*, 2002). Promoter regions were amplified from genomic DNA and introduced into the *pDONRP4P1R* vector. The coding sequences were amplified from genomic DNA or root cDNA and introduced into the *pDONR221* vector. All entry clones were sequence verified before further steps. The MYB12 promoter was subcloned into *pmK7S*nF14mGW* destination vector. The construct was transformed in Col-0 and dGR via Agrobacterium-mediated flower dipping (Clough and Bent, 1998).

Root phenotyping

For root length measurements, one-week-old roots were scanned on a flatbed scanner and root length was measured in FIJI (Schindelin *et al.*, 2012) with the integrated NEURONJ plugin (https://imagescience.org/meijering/software/neuronj/) (Meijering *et al.*, 2004). Root width of one-week-old seedlings were measured by dissecting the roots and mounting them in clearing agent (60 % lactic acid, 20 % glycerol and 20 % H_2O). Width of the root tips was measured at the beginning of the elongation zone for all roots in FIJI. Imaging of differentiated primary xylem vessels was performed on one-week-old roots mounted in the clearing agent described above. GUS staining of p*MYB12*::GUS was performed as described previously (De Rybel *et al.*, 2010). The slides were imaged using a Differential Interference contrast (DIC) microscope (Olympus BX51) equipped with a Nikon camera and image captured with ToupView software.

Statistics and visualization of the data

All boxplots and statistical analysis were generated and performed within R studio (R Core Team, 2020). In these plots, the boxes indicate the descriptive statistics with the interquartile range (IQR) with the central black line marking the median, and the 25th and 75th percentile of the data, the whiskers extend to minima and maxima within 1.5 IQR of the 25th and 75th percentiles, and outliers are indicated as single empty circles. Additionally, the means (blue rhombus) and a measure of their precision (blue standard error bars) as well as the compact letter display (blue letters) are displayed. The ‘n’ represents the number of data points, which are plotted as the grey dots. For the continuous variables, root width and root

length, one-way or two-way analysis of variance (ANOVA) with post-hoc Tukey testing at 5% level of significance was performed. Significances asterisks: * = p-value < 0.05; ** = p-value < 0.01; *** = p-value < 0.001. A generalized linear model with log link function has been fitted to count data (e.g. number of cell files). The lower-case letters (compact letter display) associated to the mean and its precision within the boxplots, indicate which groups with any common letter are not significantly different, determined by pairwise comparisons of estimated marginal means testing with p-value adjustment. P-values have been adjusted for multiple testing by the Bonferroni method, if not otherwise specified in Table S1.

Confocal imaging and processing

Transcriptional and translational fluorescent reporter lines were imaged on a Leica SP8 confocal microscope with a 40x NA 1.1 water immersion objective. Seedlings were mounted in propidium iodide (PI); GFP and sYFP reporter lines were excited at 488, resp. 514 nm and detected at 500-535, resp. 515-550 nm; PI was detected at 600-700 nm. For the vascular cell file number measurements in root tips, one-week-old seedlings were fixed and stained using the mPS-PI protocol and imaged using the Leica SP2 or SP8 confocal microscopes as described previously (Arents *et al.*, 2022; Truernit *et al.*, 2008). For the vascular cell file number of the late primary root and secondary root, 4-day, 14-day or 21-day old seedlings were used respectively. Roots were sampled 0,5 cm below the hypocotyl and vibratome cross-sections were made as described previously (Arents *et al.*, 2022). Cell walls were stained with calcofluor and lignin in xylem vessels was stained with basic fuchsin as described before (Ursache *et al.*, 2018). Cell counting was done using the cell counter plugin in FIJI (Schindelin *et al.*, 2012). The vascular bundle cell number quantifications included the pericycle cell layer, except if mentioned otherwise. The analysis of CK treated *pMYB12::*nGFP/GUS was the sum of 10 Z-slices and measured Integrated density of the whole image using FIJI (Schindelin *et al.*, 2012). All figures were assembled and processed using Inkscape and Adobe Illustrator.

RNA isolation and qRT-PCR

For dGR induction, plants were grown on ½ MS (1% agar) for 5 days before transferring to either mock or 10 μM DEX for 2h. For CK treatment, 5-day-old seedlings were transferred to medium containing 10 μM 6-benzylaminopurine (6-BAP; Duchefa) from a 10 mM DMSO stock solution. All samples were ground in liquid nitrogen and RNA was extracted using RNA isolation protocol for non-fiberous tissue by the RNA Tissue Miniprep System (Promega). cDNA synthesis was done using 1μg of total RNA with the qScriptTM cDNA Supermix kit (Quanta BioSciences). The qRT-PCR primers were designed by Universal Probe Library Design Center (Roche) (Table S3). The qRT-PCR was performed using *UBC* and *EEF* as reference genes on a Roche Lightcycler 480 device (Roche Molecular Systems Inc.) with SYBR Green I Master kit (Roche). The gene expression analysis was done using qBase v3.2 software (Biogazelle, Zwijnaarde, Belgium - www.qbaseplus.com).

DNA extraction and genotyping

Genomic DNA was isolated using the CTAB extraction method. The T-DNA mutants (*myb11*/SALK077068 and *myb111*/GK291D01) were genotyped using PCR based method (Table S3). The *myb12-1f* mutant (Mehrtens *et al.*, 2005) was genotyped using cleaved

amplified polymorphic sequence (CAPS). An amplicon of 547 bp was amplified (using primers described in Table S3), and was cut by using HphI restriction. The wild type allele was cut into two bands of 399 bp and 148 bp, while the mutant remained uncut.

Tobacco infiltration and co-immunoprecipitation

Nicotiana benthamiana leaves (3 to 4 week old) were infiltrated with a mixture of 4 C58C1Rif (pMP90) *Agrobacterium* strains containing the following constructs: *p35S::P19*, *p35S::TMO5:3xHA, p35S::LL1:3xHA* and *pUBI10-XVE-p35Sminimal:MYB12:GFP*. Leaves were harvested and immediately snap frozen by immersion in liquid nitrogen and stored at -70°C until further processing. Frozen leaves were ground with pestle and mortar until a fine powder was obtained. The ground tissue was then dissolved in extraction buffer (50mM Tris – 300mM NaCl – 5mM DTT – 1mM PMSF – pH 7.4 supplemented with proteinase inhibitor tablets 1 per 50ml of buffer) and sonicated (3x15sec on, 3x 15sec off). For each gram of plant material, 3ml of extraction buffer was used. After sonication the sample was kept on ice for 15 min and centrifuged for 2x15 min at 20.000 rcf. 100µl of anti-GFP magnetic beads (Chromotek – catalogue number: gtm-20) were added to the supernatant and incubated for 2h at 4°C on a rotating wheel. After incubation, the beads were removed from the sample and thoroughly washed with extraction buffer. Elution was performed by adding 25µl boiling sample buffer and boiling for another 10 min. Upon SDS-PAGE and Western blotting, detection was performed with 1/5000 anti-HA-HRP antibodies (Abcam, catalogue number ab1190).

Yeast-2-Hybrid (Y2H) analysis

The *MYB12, TMO5 and LHW* coding sequences were cloned into *pDEST22* (Prey: GAL4AD-x Yeast selection marker: TRP1) and *pDEST32* (Bait: GAL4DB-y Yeast selection marker: LEU2). These plasmids were transformed into *Saccharomyces cerevisiae* strain AH109 (Clontech). At least 3 independent yeast transformants were checked for each pairwise interaction according to (Cuellar *et al.*, 2013) with minor modifications: the protein-protein interactions were validated with undiluted overnight yeast culture droplets manually pipetted on selective SD Base-Leu/-Trp/-His and grown for 3-4 days at 30°C before imaging.

Knock sideways

The knock sideways (KSD) assay was performed as described previously (Winkler *et al.*, 2021). Briefly, *N. benthamiana* leaves were transiently co-transformed with the constructs *p35S::TMO5-EGFP-FKBP*, *p35S::MITO-FRB*, and *pG1090::XVE>>MYB12-TagBFP2* or p35S::TagBFP2 as a negative control. After 2 days, the transformed leaves were infiltrated with 1 µM rapamycin or H_2O mock control and images were acquired 2-4 h thereafter on a Leica SP8X or Zeiss LSM880 confocal microscope in line sequential scanning mode. The p*G1090::XVE>>MYB12-TagBFP2* construct was originally intended for estradiol-inducible expression, but turned out very leaky in expression in the *N. benthamiana* system and was thus used for constitutive expression instead.

Results

A mutant screen identifies modulators of TMO5/LHW activity

In order to identify novel regulators of TMO5/LHW activity leading to vascular proliferation via control of oriented cell divisions, we designed an EMS-based forward genetic screen in the previously described dexamethasone (DEX)-inducible p*RPS5A*::TMO5:GR x p*RPS5A*::LHW:GR double misexpression line (double GR or dGR) in Col-0 background (Smet *et al.*, 2019). Upon exogenous DEX treatment, root apical meristem width is increased in this line due to the ectopic periclinal and radial cell divisions (De Rybel *et al.*, 2013), protoxylem differentiation is inhibited due to increased cytokinin levels (De Rybel *et al.*, 2014) and additionally, primary root length is reduced (De Rybel *et al.*, 2013) (Fig. 1A-H, Table S1). We reasoned those mutations in positive/negative regulators of the TMO5/LHW pathway would suppress/enhance these dGR phenotypes. Although the TMO5/LHW activity was previously shown by a detailed quantification of the vascular cell file number (Arents *et al.*, 2022; Wendrich *et al.*, 2020; Yang *et al.*, 2021), such experiments are labour intensive and require fixed samples, making them incompatible with high-throughput screening. We thus first evaluated whether root length and meristem width could serve as reliable read-outs for TMO5/LHW activity and hence cell proliferation capacity by plotting the root length or root width parameters against the total number of quantified cell files in multiple transgenic lines with increasing levels of TMO5/LHW heterodimer activity (Col-0, p*RPS5A*::LHW:GR, p*RPS5A*::TMO5:GR, the inducible dGR line and a constitutive double TMO5/LHW misexpression line). We observed a clear inverse correlation between root length and TMO5/LHW activity and a positive correlation between root width and TMO5/LHW activity (Fig. 1I-J, Table S1). These results suggest that root length and width can serve as reliable proxies for the number of cell file number and thus TMO5/LHW activity.

Having established the screening strategy, we performed EMS mutagenesis of dGR seeds and screened 228 pools of EMS mutagenized M_2 dGR seedlings for alterations in root length upon DEX induction. This first round of selection yielded 310 candidate mutants from 110 pools, of which 260 produced viable M_3 seeds. In total, 50 albino plants were observed among these 228 pools of mutants, suggesting that the EMS mutagenesis was successful (Micol-Ponce *et al.*, 2014). In the M_3 generation, we quantified both root length and root meristem width of the 260 candidate mutants (Fig. 2A), resulting in 20 validated mutants with reduced responses (*insensitive 1-20*, *ins1-20*) and 2 mutants showing hypersensitive responses (*hypersensitive 1-2*, *hyp1-2*) (Fig. S1-3, Table S1). The *insensitive* mutants are defined as not showing a change in root length and/or root meristem width upon TMO5/LHW induction (dGR on DEX) compared to the non-induced control (dGR on mock). The *hypersensitive* mutants are defined as having an even more pronounced change in root length and/or root meristem width upon TMO5/LHW induction (dGR on DEX) compared to the non-induced control (dGR on mock). We next performed a detailed quantification of the vascular cell file number as the read-out of TMO5/LHW activity used previously (De Rybel *et al.*, 2014; De Rybel *et al.*, 2013; Ohashi-Ito and Bergmann, 2007; Ohashi-Ito *et al.*, 2013; Ohashi-Ito *et al.*, 2014). Notably, 5 insensitive mutants already showed a significantly reduced number of vascular cell files in mock conditions

compared to the non-induced control (dGR) (Fig. 2B, Table S1), suggesting that these mutants might inherently have differential TMO5/LHW activity and further confirming that our multi-step screening procedure using root length and width as proxies was successful. A segregation analysis further showed that the observed phenotypes in *ins2* and *ins7* could not be explained by a recessive mutation at a single locus (Table S2). These mutants were therefore excluded from further analysis. We finally focussed our attention on the mutants with the most pronounced phenotype in each category: *ins4* and *hyp2* (Fig. 2B, Fig. S1, Table S1), and mapped the causal mutations by next generation sequencing.

A strong lhw allele is causal to the ins4 phenotype

The insensitive *ins4* mutant (in dGR background) showed a strong reduction in the number of vascular cell files under mock condition and a repression of the increased root thickness upon DEX treatment (Fig. 2B, Fig. S1, Table S1). Indeed, upon TMO5/LHW induction in *ins4*, the number of vascular cell files increased compared to mock, but the response of *ins4* on DEX did not differ from dGR on mock (Fig S4A-B, Table S1). Sequencing and SHORE map analysis (Schneeberger *et al.*, 2009) focusing on the reduced vascular cell files phenotype under mock conditions revealed that *ins4* carried a premature stop codon in *LHW* (Fig. 3A) which was confirmed using Sanger sequencing. Similar to the published *lhw* mutant alleles (De Rybel *et al.*, 2013; Ohashi-Ito and Bergmann, 2007; Ohashi-Ito *et al.*, 2013; Parizot *et al.*, 2008), the *ins4* mutant showed a monarch vascular architecture in the primary root meristem, resulting in an off-centre xylem bundle during secondary growth (Fig. 3B-H, Table S1). The number of vascular cell files could also be rescued by exogenous cytokinin application (Fig. 3I, Table S1) as was shown before to bypass the TMO5/LHW dependent cytokinin biosynthesis (De Rybel *et al.*, 2014). It is counter intuitive that dGR induction could not rescue the *ins4* mutant while ectopic cytokinin treatment could, as both treatments converge on increased CK levels. Thus, we explored *LOG4* expression levels upon dGR induction in the *ins4* mutant background and found these were not changed to the extent seen in the dGR control (Fig. S4C). This suggests that within the *ins4* mutant background, dGR is incapable of increasing cytokinin levels, explaining the discrepancy between the dGR induction and cytokinin treatment experiments in *ins4*. It is however unclear whether this is due to the truncated LHW protein or caused by another independent mutation. Taken together, the mapping and phenotypic characterization show that *ins4* is a novel, strong *lhw* allele. We thus termed *ins4* as *lhw-8*. Although *ins4/lhw-8* itself does not provide new insight into the regulation of TMO5/LHW activity, it further confirms that our screening and mapping set-up was successful to uncover causative EMS mutations.

hyp2 is a novel myb12 allele

At the other side of the selected mutant spectrum, the recessive *hyp2* mutant showed no clear phenotype under normal growth conditions, but a strong hypersensitive response upon DEX treatment (Fig. 2B, Fig. 4N, Fig. S1, Fig. S5-7, Table S1). SHORE map analysis (Schneeberger *et al.*, 2009) identified an early stop codon in the gene encoding the R2R3 transcription factor MYB12 (Fig. 4A). To confirm the causality of the *MYB12* mutation for the observed dGR hypersensitive phenotype, we first crossed the previously published *myb11 myb12-1f myb111* triple mutant (Stracke *et al.*, 2007) into our dGR parental line. The triple mutant was chosen as at least the closely related *myb111* is also dGR inducible

(Figure S8C) (Smet *et al.*, 2019). A hypersensitive response comparable to *hyp2* was detected in the *myb11 myb12-1f myb111* dGR mutant (Fig. 4B-I, N, Table S1). This triple mutant also did not show an aberrant phenotype under mock conditions in the Col-0 control background (Fig. 4B, H, N, Table S1). Collectively, this data also suggests that MYB12 acts as a repressor of ectopically induced TMO5/LHW vascular proliferation. To further test this hypothesis, we introduced a construct driving the *MYB12* coding sequence from the strong meristematic *RPS5A* promoter (Weijers *et al.*, 2001) in the *hyp2* mutant background. p*RPS5A*::*MYB12* lines with increased *MYB12* levels showed mild repression of the number of vascular cell files already in mock conditions (Fig. S8A-B, Table S1). Upon DEX treatment, the p*RPS5A*::*MYB12* construct strongly repressed the TMO5/LHW-induced vascular cell proliferation (Fig. 4J-N, Table S1). Taken together, *hyp2* is a novel mutant allele of *MYB12*, which we designated as *myb12-2*. Our initial results hint towards a new function for this TF and suggest that MYB12 might act as a negative regulator of the TMO5/LHW pathway.

We previously found that *MYB12* is transcriptionally upregulated upon TMO5/LHW induction in the dGR line (Smet *et al.*, 2019) (Fig. 5A). We thus introduced the previously described *MYB12* transcriptional reporter (Stracke *et al.*, 2007) into the dGR line and observed increased activity of the *MYB12* promoter in the root differentiation zone upon dGR induction (Fig. S9A-B). Similar increase in expression levels upon TMO5/LHW induction in the dGR background was observed in newly generated p*MYB12*::nGFP/GUS and p*MYB12*::gMYB12:sYFP reporter lines based on the full genomic fragment of *MYB12* including the introns and a longer promoter sequence (Fig. S9C-F). Given the slow induction kinetics compared to direct TMO5/LHW target genes such as *LOG4* (Fig. 5A) (De Rybel *et al.*, 2014; Ohashi-Ito *et al.*, 2014), we hypothesized that the induction of *MYB12* is likely indirect and possibly triggered by cytokinin signalling downstream of TMO5/LHW (De Rybel *et al.*, 2014; Ohashi-Ito *et al.*, 2014). Indeed, we found *MYB12* to be cytokinin inducible by qRT-PCR analysis (Fig. 5B, Table S1), confirming previous reports (Brenner and Schmulling, 2012). Analysis of the newly generated *pMYB12::nGFP/GUS* reporter line further revealed that ectopic cytokinin treatment results in higher activity of the *MYB12* promoter (Fig. S9G-I). These results suggest that *MYB12* might be part of a negative feedback loop where TMO5/LHW, via increased cytokinin signalling, activates its own repressor to modulate vascular proliferation rates.

MYB12 represses TMO5/LHW transcriptional activity

One possible way how MYB12 could repress the TMO5/LHW activity downstream of the cytokinin response would be to alter the cytokinin response itself. To test this hypothesis, we analysed the inhibition of root length caused by increasing concentrations of exogenously applied cytokinin in *myb12* mutants. No major differences in cytokinin sensitivity were observed between either *myb12* allele and their respective control lines under mock conditions (Col-0 for *myb12-1f* and dGR for *hyp2/myb12-2*) (Fig. S11, Table S1), suggesting the repression of TMO5/LHW activity does not act at the level of cytokinin signalling or perception. Next, we tested possible repression at the level of the activity of the TMO5/LHW heterodimer itself by analysing the expression levels of direct TMO5/LHW target genes in the *hyp2/myb12-2* and p*RPS5A*::MYB12 *hyp2/myb12-2* dGR lines in

comparison to the dGR control. The expression levels of the direct target genes *LOG4* and *GH10* can be used as molecular read-out of TMO5/LHW activity (De Rybel *et al.*, 2014; Ohashi-Ito *et al.*, 2014; Vera-Sirera *et al.*, 2015). Upon DEX treatment, relative expression levels of *LOG4* and *GH10* were induced in control (dGR) and *hyp2/myb12-2* in dGR backgrounds (Fig. 5C, Table S1). In the p*RPS5A*::MYB12 *hyp2/myb12-2* dGR line, however, no induction in *LOG4* and *GH10* expression was observed (Fig. 5C, Table S1), suggesting that MYB12 might directly inhibit TMO5/LHW activity. To verify these results, we next introduced the transcriptional reporter of *LOG4* (De Rybel et al., 2014) and a newly generated reporter for *GH10* into the p*RPS5A*::MYB12 *hyp2/myb12-2* dGR line and the parental dGR line as control. Both the p*LOG4*::n3GFP and p*GH10*::n3GFP transcriptional reporters showed a clear induction in expression strength and ectopic expression upon DEX treatment in dGR/+ background compared to a mock DMSO treatment (Fig. 5D-E, H-I). This induction was repressed in the p*RPS5A*::MYB12/+ *hyp2/+* dGR/+ background (Fig. 5F-G, J-K); confirming the qRT-PCR results (Fig. 5C, Table S1). Taken together, these results suggest that MYB12 represses TMO5/LHW activity by inhibiting direct target gene expression. Importantly, MYB12 does not contain a characteristic EAR motif associated with transcriptional repressors (Kagale and Rozwadowski, 2011; Liu *et al.*, 2015) and directly activates transcription of the *CHS* and *FLS* genes (Mehrtens *et al.*, 2005). This shows that MYB12 is thus not a typical transcriptional repressor, but represses TMO5/LHW transcriptional activity in another way.

MYB12 non-competitively binds to TMO5

TMO5/LHW activity is known to be repressed by the SACL bHLH proteins, which compete with TMO5 for binding to LHW and thus reduce the amount of active TMO5/LHW dimers (Katayama *et al.*, 2015; Vera-Sirera *et al.*, 2015). Given the well documented interactions between MYB and bHLH TFs (Carretero-Paulet *et al.*, 2010; Cui *et al.*, 2021; Feller *et al.*, 2011; Zhao *et al.*, 2008), we hypothesized that MYB12 function might involve direct binding to the TMO5/LHW complex (Katayama *et al.*, 2015; Vera-Sirera *et al.*, 2015). Firstly, if MYB12 were to bind the TMO5/LHW complex, it would need to be present in the same cells. As single-cell transcriptomics (Wendrich *et al.*, 2020) suggested a broader *MYB12* meristematic expression domain than revealed by the existing *MYB12* transcriptional reporter (Stracke *et al.*, 2007) (Fig. S9a, Fig. S10A), we speculated that additional regulatory elements might be present in the *MYB12* coding region. To this end, we more closely examined our newly generated reporter lines (Fig. 6A-D, Fig. S10B). In agreement with previous findings (Stracke *et al.*, 2007; Struk *et al.*, 2022), the expression was the strongest in most cells from the elongation zone onwards, including xylem cells, and in the lateral root cap. Nonetheless, our genomic fusion containing introns and a longer promoter region revealed additional *MYB12* expression also in epidermis, cortex, and importantly, xylem cells of the meristematic zone (Fig. S10B), confirming the recently published single cell transcriptomic data (Wendrich *et al*, 2020) (Fig. S10A). It is thus conceivable that MYB12 could directly interact with the TMO5/LHW complex, expressed in xylem cells throughout the root meristem as driven from their endogenous promoters (Fig. 6, S9-10) (De Rybel *et al.*, 2013).

We therefore next tested the capacity of MYB12 to directly interact with TMO5 and/or LHW. Yeast-2-Hybrid (Y2H) analysis showed that MYB12 is able to bind to TMO5 (Fig. 7A). Binding of MYB12 to LHW could not be evaluated due to auto-activation of LHW-BD and MYB12-BD in the yeast system (Fig. S12). This could be caused by the innate transcriptional activity of LHW and MYB12. We next performed co-immunoprecipitation and could confirm the interaction between TMO5-HA and MYB12-GFP. Additionally, a putative interaction between MYB12-GFP and LHW-LIKE1-HA was found (Fig. 7B, S13). To provide additional confirmation of these interactions *in planta* using an independent system, we took advantage of the recently developed rapamycin-dependent knock sideways assay in transiently transformed *N. benthamiana* leaves (Winkler *et al.*, 2021). This assay is based on the ability of FKBP and FRB protein domains to solely dimerize in presence of the drug rapamycin (Belshaw *et al.*, 1996). In control conditions, we observed that simultaneous infiltration of plasmids carrying TMO5-GFP-FKB, MYB12-TagBFP2 and a mitochondria-targeted FRB resulted in nuclear localization of the TMO5 and MYB12 fusions, as expected from transcription factors (Fig. 7C). In the presence of rapamycin, TMO5-GFP-FKBP bound to mito-FRB and delocalized to the mitochondria (Fig. 7D). Together with TMO5-GFP-FKBP, MYB12-TagBFP2, but not free TagBFP2, co-translocalized towards the mitochondria (Fig. 7C-D), indicating that TMO5 interacted with MYB12. Taken together, these experiments show that TMO5, and perhaps LHW homologs, can directly interact *in vivo* and *in planta* with MYB12. This corresponds with previous findings where MYB transcription factors are part of the bHLH/MYB/WD40 complex (Ramsay and Glover, 2005).

Altogether, using forward genetics, we have identified the R2R3 MYB transcription factor MYB12 as a novel regulator of the TMO5/LHW pathway during root vascular proliferation. MYB12 directly interacts with TMO5 and represses the activity of the TMO5/LHW complex at the level of direct target gene expression. *MYB12* itself is a downstream target gene of the TMO5/LHW pathway, thus constituting a negative feedback loop which contributes to fine tuning the activity of the TMO5/LHW complex during vascular development in the root meristem.

Discussion

The patterning and proliferation of the vascular bundle during primary root growth relies on a complex regulatory network of transcriptional, hormonal and other signals (De Rybel *et al.*, 2016). The key heterodimeric bHLH transcription factor complex, TMO5/LHW, promotes cytokinin biosynthesis via promoting the expression of *LOG3*, *LOG4* and *BGLU44* in the xylem cells (De Rybel *et al.*, 2014; Ohashi-Ito *et al.*, 2014; Yang *et al.*, 2021). This locally produced cytokinin is thought to act as a mobile signal that coordinates the radial growth and correct patterning of the vascular bundle (Wybouw and De Rybel, 2019). In this study, we have taken a forward genetic approach to find new regulators of the TMO5/LHW pathway and discovered a novel function of the previously described transcription factor MYB12. Our data revealed that *myb12* mutants are hypersensitive to the gain-of-function phenotypes caused by TMO5/LHW misexpression, while *MYB12* misexpression represses vascular proliferation by inhibiting the transcriptional activation of direct TMO5/LHW targets genes. Moreover, *MYB12* is transcriptionally activated by the

cytokinin response downstream of TMO5/LHW, and MYB12 directly interacts with TMO5 and possibly LHW homologs. All these findings indicate that MYB12 acts as a repressor of the *TMO5/LHW* transcriptional pathway, while at the same time being its downstream target. Hence, we have found a novel negative feedback loop regulating the TMO5/LHW transcriptional network via the action of MYB12.

This negative feedback loop is reminiscent of the previously described regulation of the TMO5/LHW pathway by the *SACL* genes. Nonetheless, there are several key differences between the MYB12- and SACL-mediated negative feedback loops. Firstly, *MYB12* appears to be a secondary TMO5/LHW target induced indirectly by the downstream cytokinin response, while the *SACL* genes are direct targets of TMO5/LHW (Katayama *et al.*, 2015; Vera-Sirera *et al.*, 2015). This would suggest that the MYB12-mediated negative feedback is slower in comparison to the SACL loop, which might be important for spatiotemporal fine tuning TMO5/LHW activity. Furthermore, the cytokinin response levels are affected by numerous factors other than TMO5/LHW (Kieber and Schaller, 2018). Thus, the cytokinin-inducible MYB12 can, unlike the SACL proteins, help optimize vascular proliferation rates by integrating the TMO5/LHW activity with other developmental signals. In support of the SACL- and MYB12-mediated negative feedback loops acting on different spatiotemporal scales, *SACL* and *MYB12* have very distinct expression patterns. *SACL*s are co-expressed with *TMO5* and *LHW* in all xylem cells in the root meristem zone (Vera-Sirera *et al.*, 2015). *MYB12* is most prominently expressed in older root tissues from the differentiation zone onwards and in the late meristematic xylem cells, consistent with providing slower and more indirect feedback. However, the SACL and MYB12 regulatory loops do not seem to be mutual exclusive, as *myb12* mutants are hypersensitive towards increased TMO5/LHW activity in the root meristem. Unfortunately, despite clear inhibitory effects on vascular proliferation in both *SACL* and *MYB12* gain-of-function lines, a lack of prominent aberrant phenotypes in the respective loss-of-function mutants makes it difficult to dissect the exact function of these genes during vascular development. This further emphasizes the pronounced genetic redundancy operating in plant development, especially during the control of such vital processes like vascular tissue patterning.

We have shown that MYB12 directly interacts with TMO5, and likely also LHW homologs and inhibits the transcriptional activation of direct TMO5/LHW target genes. Nonetheless, the exact molecular mechanism of MYB12 action remains unclear. MYB12 does not contain an EAR or TLLLFR motif typical for MYB TF repressors (Kagale and Rozwadowski, 2011; Ma and Constabel, 2019). Additionally, MYB12 lacks the bHLH-binding motif present in other known bHLH-interacting MYB TFs (Wang and Chen, 2014; Zimmermann *et al.*, 2004), and it functions as a *bona fide* transcriptional activator (Forkmann and Martens, 2001; Mehrtens *et al.*, 2005).

Therefore, the MYB12-mediated inhibition of TMO5/LHW activity must depend on another molecular mechanism. In one scenario, MYB12 might act as a passive repressor by preventing TMO5/LHW interaction with DNA and/or recruitment of the RNA polymerase II complex (Kazan, 2006; Krogan and Long, 2009). Another and more likely possibility is that, rather than acting as a conventional repressor, MYB12 might redirect TMO5/LHW activity away from *LOG4*, *GH10* and other genes involved in vascular proliferation, and

contribute to activating different TMO5/LHW target genes instead. This explanation would fit best with the previously described function of MYB12 as a classical transcriptional activator of several genes in the flavonoid biosynthesis pathway (Forkmann and Martens, 2001; Mehrtens *et al.*, 2005). Target gene specificity has previously been associated with the MYB TFs in heteromeric bHLH-MYB transcriptional complexes (Ramsay and Glover, 2005). TMO5-LIKE 1 (T5L1), a close homolog of TMO5, is able to promote ectopic xylem differentiation in addition to its role in promoting radial growth (Katayama *et al.*, 2015); The same bHLH TF thus functions in two very different developmental processes that require the activation of completely different gene sets. It is conceivable that such alternative functionalities of bHLH TFs could be achieved by interactions with different MYBs. In such a scenario, the TMO5/LHW complex would recruit an unknown MYB TF to promote the expression of genes required for vascular proliferation, while the alternative recruitment of MYB12 would lead to the activation of different target genes. To take this speculation even further, the dual roles of MYB12 in flavonol biosynthesis (Forkmann and Martens, 2001; Mehrtens *et al.*, 2005) and vascular proliferation (this study) could then be explained by alternative interactions with TMO5 and an unknown bHLH TF needed for MYB12-mediated induction of the *CHS* and *FLS* flavonol biosynthesis genes. Further investigations into the precise molecular mechanisms responsible for MYB12 as well as other related MYB TFs action will be needed to shed light on these intriguing open questions and hypotheses.

What is the biological meaning of the same transcription factor MYB12 being involved in flavonol biosynthesis as well as vascular proliferation is another open question arising from our study. Interestingly, the bHLH TF TRANSPARENT TESTA 8 (TT8) has been previously implied in flavonoid biosynthesis (Nesi *et al.*, 2000) and trichome development (Maes *et al.*, 2008), indicating that dual functions in different metabolic and developmental pathways might be a common feature of multiple transcription factors from different families (Zhang *et al.*, 2017). This might reflect the need of certain metabolic changes for a specific developmental process. For example, trichomes are rich in biotic stress defence compounds which include flavonoids (Karabourniotis *et al.*, 2020). Utilizing TT8 to control both trichome development and flavonoid biosynthesis might thus aid in coordinating the two processes. Likewise, the transition from vascular proliferation to differentiation might involve so far unappreciated metabolic changes in addition to the decline of TMO5/LHW activity, both hypothetically controlled by MYB12. Alternatively, dampening the TMO5/LHW pathway while promoting flavonoid biosynthesis might contribute to the balance between growth and defence processes. Different stresses often lead to increased reactive oxygen species levels, which can be mitigated by flavonoid antioxidant activity (Wang *et al.*, 2016). In such conditions, attenuating the TMO5/LHW-mediated radial growth in favour of flavonoid biosynthesis by the increased MYB12 levels could be important for optimal resource allocation.

In summary, we have uncovered a novel role of the transcription factor MYB12 as a negative regulator of the TMO5/LHW pathway during vascular proliferation. The MYB12-mediated negative feedback loop is distinct from the modus operandi of the previously described SACL proteins in both molecular mechanism and spatiotemporal dynamics, showing that TMO5/LHW activity is being controlled using multiple distinct mechanisms. The full molecular details of MYB12 mode of action, as well as the biological meaning of its dual

functions in vascular development and flavonoid biosynthesis, remain exciting challenges for future investigations. Our work establishes that a *bona fide* transcriptional activator can function as a repressor in a different transcriptional network. Furthermore, our results show that functional interactions between bHLH and MYB transcription factors are involved in multiple unrelated transcriptional networks, highlighting them as a powerful and possibly underappreciated developmental module.

Supplementary Material

Refer to Web version on PubMed Central for supplementary material.

Acknowledgements

The authors thank Ralf Stracke and Sofie Goormachtig for sharing the *myb11myb12-1f,myb111* and *myb12-f* mutant seeds, respectively; Davy Opdenacker for help with the EMS mutagenesis and Frederik Coppens for help with the SHOREmap analysis. B.D.R. would like to thank T.G.A. and A.P.M. for helpful discussions completely unrelated to this work.

Funding

This work was funded by The Research Foundation - Flanders (FWO; Odysseus II G0D0515N and post-doc fellowship 1215820N); the Netherlands Organization for Scientific Research (NWO; VIDI 864.13.00); the European Research Council (ERC Starting Grant TORPEDO; 714055); the European Union's Horizon 2020 research and innovation programme under the Marie Sklodowska-Curie grant agreement No 885979 "DIVISION BELL"; EMBO (long term fellowship ALTF 1005-2019); and ERC consolidator Grant T-REX; 682436 to DVD; ERC Starting Grant COSI; 949808 to I.D.C and the China Scholarship Council (PhD fellowship 201706910099) to X.L..

Data availability

All data supporting the findings of this study and respective statistics are available within the paper in Table S1. Materials and resources of this study are available from the corresponding author upon reasonable request.

References

Appelhagen I, Jahns O, Bartelniewoehner L, Sagasser M, Weisshaar B, Stracke R. Leucoanthocyanidin Dioxygenase in Arabidopsis thaliana: characterization of mutant alleles and regulation by MYB-BHLH-TTG1 transcription factor complexes. Gene. 2011; 484: 61–68. [PubMed: 21683773]

Arents HE, Eswaran G, Glanc M, Mahonen AP, De Rybel B. Means to Quantify Vascular Cell File Numbers in Different Tissues. Methods in Molecular Biology. 2022; 2382: 155–179. [PubMed: 34705239]

Belshaw PJ, Ho SN, Crabtree GR, Schreiber SL. Controlling protein association and subcellular localization with a synthetic ligand that induces heterodimerization of proteins. Proceedings of the National Academy of Sciences U S A. 1996; 93: 4604–4607.

Europe PMC Funders Author Manuscripts

Brenner WG, Schmulling T. Transcript profiling of cytokinin action in Arabidopsis roots and shoots discovers largely similar but also organ-specific responses. BMC Plant Biology. 2012; 12: 112. [PubMed: 22824128]

Carretero-Paulet L, Galstyan A, Roig-Villanova I, Martinez-Garcia JF, Bilbao-Castro JR, Robertson DL. Genome-wide classification and evolutionary analysis of the bHLH family of transcription factors in Arabidopsis, poplar, rice, moss, and algae. Plant Physiology. 2010; 153: 1398–1412. [PubMed: 20472752]

Clough SJ, Bent AF. Floral dip: a simplified method for Agrobacterium-mediated transformation of Arabidopsis thaliana. the Plant Journal. 1998; 16: 735–743. [PubMed: 10069079]

Cuellar AP, Pauwels L, De Clercq R, Goossens A. Yeast two-hybrid analysis of jasmonate signaling proteins. Methods in Molecular Biology. 2013; 1011: 173–185. [PubMed: 23615996]

Cui D, Zhao S, Xu H, Allan AC, Zhang X, Fan L, Chen L, Su J, Shu Q, Li K. The interaction of MYB, bHLH and WD40 transcription factors in red pear (Pyrus pyrifolia) peel. Plant Molecular Biology. 2021; 106: 407–417. [PubMed: 34117570]

De Rybel B, Adibi M, Breda AS, Wendrich JR, Smit ME, Novak O, Yamaguchi N, Yoshida S, Van Isterdael G, Palovaara J, Nijsse B, et al. Plant development. Integration of growth and patterning during vascular tissue formation in Arabidopsis. Science. 2014; 345 1255215 [PubMed: 25104393]

De Rybel B, Mahonen AP, Helariutta Y, Weijers D. Plant vascular development: from early specification to differentiation. Nature Reviews Molecular Cell Biology. 2016; 17: 30–40. [PubMed: 26580717]

De Rybel B, Moller B, Yoshida S, Grabowicz I, Barbier de Reuille P, Boeren S, Smith RS, Borst JW, Weijers D. A bHLH complex controls embryonic vascular tissue establishment and indeterminate growth in Arabidopsis. Developmental Cell. 2013; 24: 426–437. [PubMed: 23415953]

De Rybel B, Vassileva V, Parizot B, Demeulenaere M, Grunewald W, Audenaert D, Van Campenhout J, Overvoorde P, Jansen L, Vanneste S, Moller B, et al. A novel aux/IAA28 signaling cascade activates GATA23-dependent specification of lateral root founder cell identity. Current Biology. 2010; 20: 1697–1706. [PubMed: 20888232]

Du H, Zhang L, Liu L, Tang XF, Yang WJ, Wu YM, Huang YB, Tang YX. Biochemical and molecular characterization of plant MYB transcription factor family. Biochemistry (Moscow). 2009; 74: 1–11. [PubMed: 19232042]

Dubos C, Stracke R, Grotewold E, Weisshaar B, Martin C, Lepiniec L. MYB transcription factors in Arabidopsis. Trends in Plant Science. 2010; 15: 573–581. [PubMed: 20674465]

Feller A, Machemer K, Braun EL, Grotewold E. Evolutionary and comparative analysis of MYB and bHLH plant transcription factors. the Plant Journal. 2011; 66: 94–116. [PubMed: 21443626]

Forkmann G, Martens S. Metabolic engineering and applications of flavonoids. Current Opinion in Biotechnology. 2001; 12: 155–160. [PubMed: 11287230]

Jin H, Martin C. Multifunctionality and diversity within the plant MYB-gene family. Plant Molecular Biology. 1999; 41: 577–585. [PubMed: 10645718]

Kagale S, Rozwadowski K. EAR motif-mediated transcriptional repression in plants: an underlying mechanism for epigenetic regulation of gene expression. Epigenetics. 2011; 6: 141–146. [PubMed: 20935498]

Karabourniotis G, Liakopoulos G, Nikolopoulos D, Bresta P. Protective and defensive roles of non-glandular trichomes against multiple stresses: structure-function coordination. Journal of Forestry Research. 2020; 31: 1–12.

Karimi M, Inze D, Depicker A. GATEWAY vectors for Agrobacterium-mediated plant transformation. Trends in Plant Science. 2002; 7: 193–195. [PubMed: 11992820]

Katayama H, Iwamoto K, Kariya Y, Asakawa T, Kan T, Fukuda H, Ohashi-Ito K. A Negative Feedback Loop Controlling bHLH Complexes Is Involved in Vascular Cell Division and Differentiation in the Root Apical Meristem. Current Biology. 2015; 25: 3144–3150. [PubMed: 26616019]

Kazan K. Negative regulation of defence and stress genes by EAR-motif-containing repressors. Trends in Plant Science. 2006; 11: 109–112. [PubMed: 16473545]

Kieber JJ, Schaller GE. Cytokinin signaling in plant development. Development. 2018; 145

Kirik V, Simon M, Huelskamp M, Schiefelbein J. The ENHANCER OF TRY AND CPC1 gene acts redundantly with TRIPTYCHON and CAPRICE in trichome and root hair cell patterning in Arabidopsis. Developmental Biology. 2004; 268: 506–513. [PubMed: 15063185]

Krogan NT, Long JA. Why so repressed? Turning off transcription during plant growth and development. Current Opinion in Plant Biology. 2009; 12: 628–636. [PubMed: 19700365]

Kurakawa T, Ueda N, Maekawa M, Kobayashi K, Kojima M, Nagato Y, Sakakibara H, Kyozuka J. Direct control of shoot meristem activity by a cytokinin-activating enzyme. Nature. 2007; 445: 652–655. [PubMed: 17287810]

Kuroha T, Tokunaga H, Kojima M, Ueda N, Ishida T, Nagawa S, Fukuda H, Sugimoto K, Sakakibara H. Functional analyses of LONELY GUY cytokinin-activating enzymes reveal the importance of the direct activation pathway in Arabidopsis. Plant Cell. 2009; 21: 3152–3169. [PubMed: 19837870]

Lee MM, Schiefelbein J. WEREWOLF, a MYB-related protein in Arabidopsis, is a position-dependent regulator of epidermal cell patterning. Cell. 1999; 99: 473–483. [PubMed: 10589676]

Lepiniec L, Debeaujon I, Routaboul JM, Baudry A, Pourcel L, Nesi N, Caboche M. Genetics and biochemistry of seed flavonoids. Annual Review of Plant Biology. 2006; 57: 405–430.

Liu J, Osbourn A, Ma P. MYB Transcription Factors as Regulators of Phenylpropanoid Metabolism in Plants. Molecular Plant. 2015; 8: 689–708. [PubMed: 25840349]

Ma D, Constabel CP. MYB Repressors as Regulators of Phenylpropanoid Metabolism in Plants. Trends in Plant Science. 2019; 24: 275–289. [PubMed: 30704824]

Maes L, Inze D, Goossens A. Functional specialization of the TRANSPARENT TESTA GLABRA1 network allows differential hormonal control of laminal and marginal trichome initiation in Arabidopsis rosette leaves. Plant Physiology. 2008; 148: 1453–1464. [PubMed: 18784284]

Mehrtens F, Kranz H, Bednarek P, Weisshaar B. The Arabidopsis transcription factor MYB12 is a flavonol-specific regulator of phenylpropanoid biosynthesis. Plant Physiology. 2005; 138: 1083–1096. [PubMed: 15923334]

Meijering E, Jacob M, Sarria JC, Steiner P, Hirling H, Unser M. Design and validation of a tool for neurite tracing and analysis in fluorescence microscopy images. Cytometry part A. 2004; 58: 167–176.

Micol-Ponce R, Aguilera V, Ponce MR. A genetic screen for suppressors of a hypomorphic allele of Arabidopsis ARGONAUTE1. Scientific Reports. 2014; 4 5533 [PubMed: 24985352]

Miyashima S, Roszak P, Sevilem I, Toyokura K, Blob B, Heo JO, Mellor N, Help-Rinta-Rahko H, Otero S, Smet W, Boekschoten M, et al. Mobile PEAR transcription factors integrate positional cues to prime cambial growth. Nature. 2019; 565: 490–494. [PubMed: 30626969]

Nesi N, Debeaujon I, Jond C, Pelletier G, Caboche M, Lepiniec L. The TT8 gene encodes a basic helix-loop-helix domain protein required for expression of DFR and BAN genes in Arabidopsis siliques. Plant Cell. 2000; 12: 1863–1878. [PubMed: 11041882]

Ogata K, Kanei-Ishii C, Sasaki M, Hatanaka H, Nagadoi A, Enari M, Nakamura H, Nishimura Y, Ishii S, Sarai A. The cavity in the hydrophobic core of Myb DNA-binding domain is reserved for DNA recognition and trans-activation. Nature Structural Molecular Biology. 1996; 3: 178–187.

Ohashi-Ito K, Bergmann DC. Regulation of the Arabidopsis root vascular initial population by LONESOME HIGHWAY. Development. 2007; 134: 2959–2968. [PubMed: 17626058]

Ohashi-Ito K, Fukuda H. Transcriptional networks regulating root vascular development. Current Opinion in Plant Biology. 2020; 57: 118–123. [PubMed: 32927424]

Ohashi-Ito K, Matsukawa M, Fukuda H. An atypical bHLH transcription factor regulates early xylem development downstream of auxin. Plant and Cell Physiology. 2013; 54: 398–405. [PubMed: 23359424]

Ohashi-Ito K, Saegusa M, Iwamoto K, Oda Y, Katayama H, Kojima M, Sakakibara H, Fukuda H. A bHLH complex activates vascular cell division via cytokinin action in root apical meristem. Current Biology. 2014; 24: 2053–2058. [PubMed: 25131670]

Oppenheimer DG, Herman PL, Sivakumaran S, Esch J, Marks MD. A myb gene required for leaf trichome differentiation in Arabidopsis is expressed in stipules. Cell. 1991; 67: 483–493. [PubMed: 1934056]

Otero S, Gildea I, Roszak P, Lu Y, Di Vittori V, Bourdon M, Kalmbach L, Blob B, Heo JO, Peruzzo F, Laux T, et al. A root phloem pole cell atlas reveals common transcriptional states in protophloem-adjacent cells. Nature Plants. 2022; 8: 954–970. [PubMed: 35927456]

Parizot B, Laplaze L, Ricaud L, Boucheron-Dubuisson E, Bayle V, Bonke M, De Smet I, Poethig SR, Helariutta Y, Haseloff J, Chriqui D, et al. Diarch symmetry of the vascular bundle in Arabidopsis root encompasses the pericycle and is reflected in distich lateral root initiation. Plant Physiology. 2008; 146: 140–148. [PubMed: 17993548]

R Core Team. 2020. RStudio | Open source professional software for data science teams-RStudio. Available at: https://www.rstudio.com/RStudio

Ramsay NA, Glover BJ. MYB-bHLH-WD40 protein complex and the evolution of cellular diversity. Trends in Plant Science. 2005; 10: 63–70. [PubMed: 15708343]

Schindelin J, Arganda-Carreras I, Frise E, Kaynig V, Longair M, Pietzsch T, Preibisch S, Rueden C, Saalfeld S, Schmid B, Tinevez JY, et al. Fiji: an open-source platform for biological-image analysis. Nature Methods. 2012; 9: 676–682. [PubMed: 22743772]

Schneeberger K, Ossowski S, Lanz C, Juul T, Petersen AH, Nielsen KL, Jorgensen JE, Weigel D, Andersen SU. SHOREmap: simultaneous mapping and mutation identification by deep sequencing. Nature Methods. 2009; 6: 550–551. [PubMed: 19644454]

Smet W, Sevilem I, de Luis Balaguer MA, Wybouw B, Mor E, Miyashima S, Blob B, Roszak P, Jacobs TB, Boekschoten M, Hooiveld G, et al. DOF2.1 Controls Cytokinin-Dependent Vascular Cell Proliferation Downstream of TMO5/LHW. Current Biology. 2019; 29: 520–529. e526 [PubMed: 30686737]

Song SK, Kwak SH, Chang SC, Schiefelbein J, Lee MM. WEREWOLF and ENHANCER of GLABRA3 are interdependent regulators of the spatial expression pattern of GLABRA2 in Arabidopsis. Biochemical and Biophysical Research Communications. 2015; 467: 94–100. [PubMed: 26408906]

Stracke R, Ishihara H, Huep G, Barsch A, Mehrtens F, Niehaus K, Weisshaar B. Differential regulation of closely related R2R3-MYB transcription factors controls flavonol accumulation in different parts of the Arabidopsis thaliana seedling. the Plant Journal. 2007; 50: 660–677. [PubMed: 17419845]

Stracke R, Jahns O, Keck M, Tohge T, Niehaus K, Fernie AR, Weisshaar B. Analysis of PRODUCTION OF FLAVONOL GLYCOSIDES-dependent flavonol glycoside accumulation in Arabidopsis thaliana plants reveals MYB11-, MYB12-and MYB111-independent flavonol glycoside accumulation. New Phytologist. 2010; 188: 985–1000. [PubMed: 20731781]

Stracke R, Turgut-Kara N, Weisshaar B. The AtMYB12 activation domain maps to a short C-terminal region of the transcription factor. Zeitschrift für Naturforschung C. 2017; 72: 251–257.

Stracke R, Werber M, Weisshaar B. The R2R3-MYB gene family in Arabidopsis thaliana. Current Opinion in Plant Biology. 2001; 4: 447–456. [PubMed: 11597504]

Struk S, Braem L, Matthys C, Walton A, Vangheluwe N, Van Praet S, Jiang L, Baster P, De Cuyper C, Boyer FD, Stes E, et al. Transcriptional Analysis in the Arabidopsis Roots Reveals New Regulators that Link rac-GR24 Treatment with Changes in Flavonol Accumulation, Root Hair Elongation and Lateral Root Density. Plant and Cell Physiology. 2022; 63: 104–119. [PubMed: 34791413]

Tominaga-Wada R, Kurata T, Wada T. Localization of ENHANCER OF TRY AND CPC1 protein in Arabidopsis root epidermis. Journal of Plant Physiology. 2017; 214: 48–52. [PubMed: 28437677]

Truernit E, Bauby H, Dubreucq B, Grandjean O, Runions J, Barthelemy J, Palauqui JC. High-resolution whole-mount imaging of three-dimensional tissue organization and gene expression enables the study of Phloem development and structure in Arabidopsis. Plant Cell. 2008; 20: 1494–1503. [PubMed: 18523061]

Ursache R, Andersen TG, Marhavy P, Geldner N. A protocol for combining fluorescent proteins with histological stains for diverse cell wall components. the Plant Journal. 2018; 93: 399–412. [PubMed: 29171896]

Vera-Sirera F, De Rybel B, Urbez C, Kouklas E, Pesquera M, Alvarez-Mahecha JC, Minguet EG, Tuominen H, Carbonell J, Borst JW, Weijers D, et al. A bHLH-Based Feedback Loop

Restricts Vascular Cell Proliferation in Plants. Developmental Cell. 2015; 35: 432–443. [PubMed: 26609958]

Wada T, Tachibana T, Shimura Y, Okada K. Epidermal cell differentiation in Arabidopsis determined by a Myb homolog, CPC. Science. 1997; 277: 1113–1116. [PubMed: 9262483]

Wang F, Kong W, Wong G, Fu L, Peng R, Li Z, Yao Q. AtMYB12 regulates flavonoids accumulation and abiotic stress tolerance in transgenic Arabidopsis thaliana. Molecular Genetics and Genomics volume. 2016; 291: 1545–1559.

Wang S, Chen JG. Regulation of cell fate determination by single-repeat R3 MYB transcription factors in Arabidopsis. Frontiers in Plant Science. 2014; 5: 133. [PubMed: 24782874]

Wang S, Hubbard L, Chang Y, Guo J, Schiefelbein J, Chen JG. Comprehensive analysis of single-repeat R3 MYB proteins in epidermal cell patterning and their transcriptional regulation in Arabidopsis. BMC Plant Biology. 2008; 8: 81. [PubMed: 18644155]

Weijers D, Franke-van Dijk M, Vencken RJ, Quint A, Hooykaas P, Offringa R. An Arabidopsis Minute-like phenotype caused by a semi-dominant mutation in a RIBOSOMAL PROTEIN S5 gene. Development. 2001; 128: 4289–4299. [PubMed: 11684664]

Wendrich JR, Yang B, Vandamme N, Verstaen K, Smet W, Van de Velde C, Minne M, Wybouw B, Mor E, Arents HE, Nolf J, et al. Vascular transcription factors guide plant epidermal responses to limiting phosphate conditions. Science. 2020; 370

Winkel-Shirley B. Flavonoid biosynthesis. A colorful model for genetics, biochemistry, cell biology, and biotechnology. Plant Physiology. 2001; 126: 485–493. [PubMed: 11402179]

Winkler J, Mylle E, De Meyer A, Pavie B, Merchie J, Grones P, Van Damme DL. Visualizing protein-protein interactions in plants by rapamycin-dependent delocalization. Plant Cell. 2021; 33: 1101–1117. [PubMed: 33793859]

Wybouw B, De Rybel B. Cytokinin-A Developing Story. Trends in Plant Science. 2019; 24: 177–185. [PubMed: 30446307]

Xu W, Dubos C, Lepiniec L. Transcriptional control of flavonoid biosynthesis by MYB-bHLH-WDR complexes. Trends in Plant Science. 2015; 20: 176–185. [PubMed: 25577424]

Xu W, Grain D, Le Gourrierec J, Harscoet E, Berger A, Jauvion V, Scagnelli A, Berger N, Bidzinski P, Kelemen Z, Salsac F, et al. Regulation of flavonoid biosynthesis involves an unexpected complex transcriptional regulation of TT8 expression, in Arabidopsis. New Phytologist. 2013; 198: 59–70. [PubMed: 23398515]

Yang B, Minne M, Brunoni F, Plackova L, Petrik I, Sun Y, Nolf J, Smet W, Verstaen K, Wendrich JR, Eekhout T, et al. Non-cell autonomous and spatiotemporal signalling from a tissue organizer orchestrates root vascular development. Nature Plants. 2021; 7: 1485–1494. [PubMed: 34782768]

Yperman K, Wang J, Eeckhout D, Winkler J, Vu LD, Vandorpe M, Grones P, Mylle E, Kraus M, Merceron R, Nolf J, et al. Molecular architecture of the endocytic TPLATE complex. Science Advances. 2021; 7

Zhang X, Ivanova A, Vandepoele K, Radomiljac J, Van de Velde J, Berkowitz O, Willems P, Xu Y, Ng S, Van Aken O, Duncan O, et al. The Transcription Factor MYB29 Is a Regulator of ALTERNATIVE OXIDASE1a. Plant Physiology. 2017; 173: 1824–1843. [PubMed: 28167700]

Zhao M, Morohashi K, Hatlestad G, Grotewold E, Lloyd A. The TTG1-bHLH-MYB complex controls trichome cell fate and patterning through direct targeting of regulatory loci. Development. 2008; 135: 1991–1999. [PubMed: 18434419]

Zimmermann IM, Heim MA, Weisshaar B, Uhrig JF. Comprehensive identification of Arabidopsis thaliana MYB transcription factors interacting with R/B-like BHLH proteins. the Plant Journal. 2004; 40: 22–34. [PubMed: 15361138]

Europe PMC Funders Author Manuscripts

Highlight

A forward genetics screen identifies MYB12 as a repressor of TMO5/LHW activity which ensures optimal cell proliferation rates during root vascular development.

Europe PMC Funders Author Manuscripts

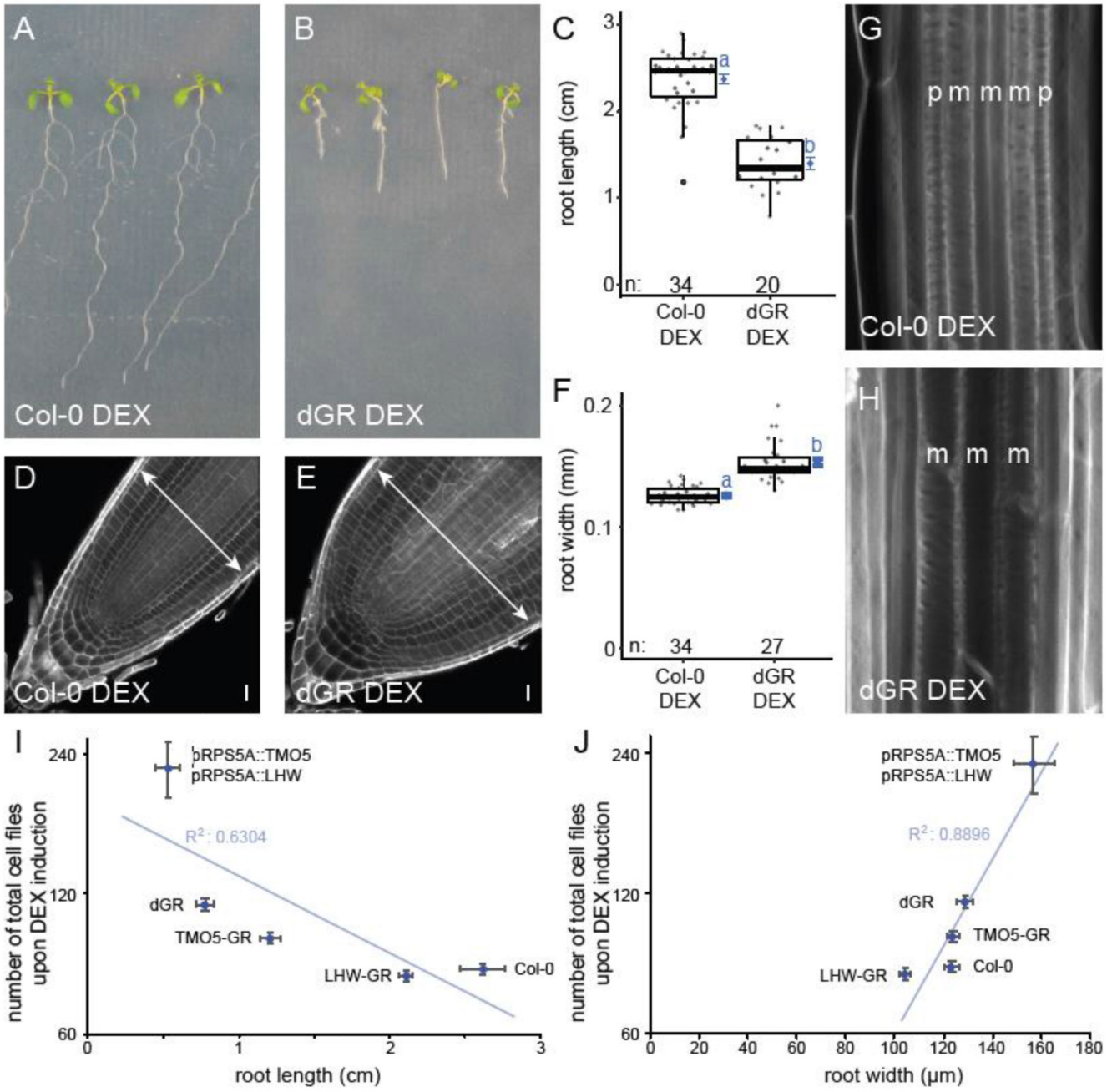

Figure 1. Root phenotype of Col-0 and the dGR line on induced (DEX) media.

(**A**-**B**) 1- week-old Col-0 (**A**) and dGR (**B**) plants grown on 10 µM DEX. (**C**) Boxplot of root length of Col-0 and dGR plants grown for 5 days on 10 µM DEX. (**D**-**E**) Col-0 (**D**) and dGR (**E**) root tips grown on 10 µM DEX. Arrows are highlighting root meristem width. (**F**) Boxplot of root width of Col-0 and dGR plants grown on 10 µM DEX. Black lines indicates the median and grey boxes indicate data ranges. The mean and its precision are plotted as the blue rhombus with blue SE bars. Blue lower-case letters (compact letter display) at these means in C, F not sharing a letter indicate significantly different groups as determined by one-way ANOVA with post-hoc Tukey testing at 5% significance level. The n marks

the number of datapoints for each sample. (**G**-**H**) The vascular differentiation phenotype of Col-0 (**G**) and dGR (**H**) plants grown on 10 μM DEX. The p and m indicate protoxylem and metaxylem strands respectively. Root width of Col-0 and dGR plants grown for 5 days on 10 μM DEX ($n \geq 20$). (**I**-**J**) 1-week old seedlings grown on 10 μM DEX ($n \geq 10$), were used to plot the number of total cell files in the root meristem against the root length (**I**) or root width (**J**). Error bars indicate standard error. Scale bars in D-E indicate 10 μm.

Europe PMC Funders Author Manuscripts

Europe PMC Funders Author Manuscripts

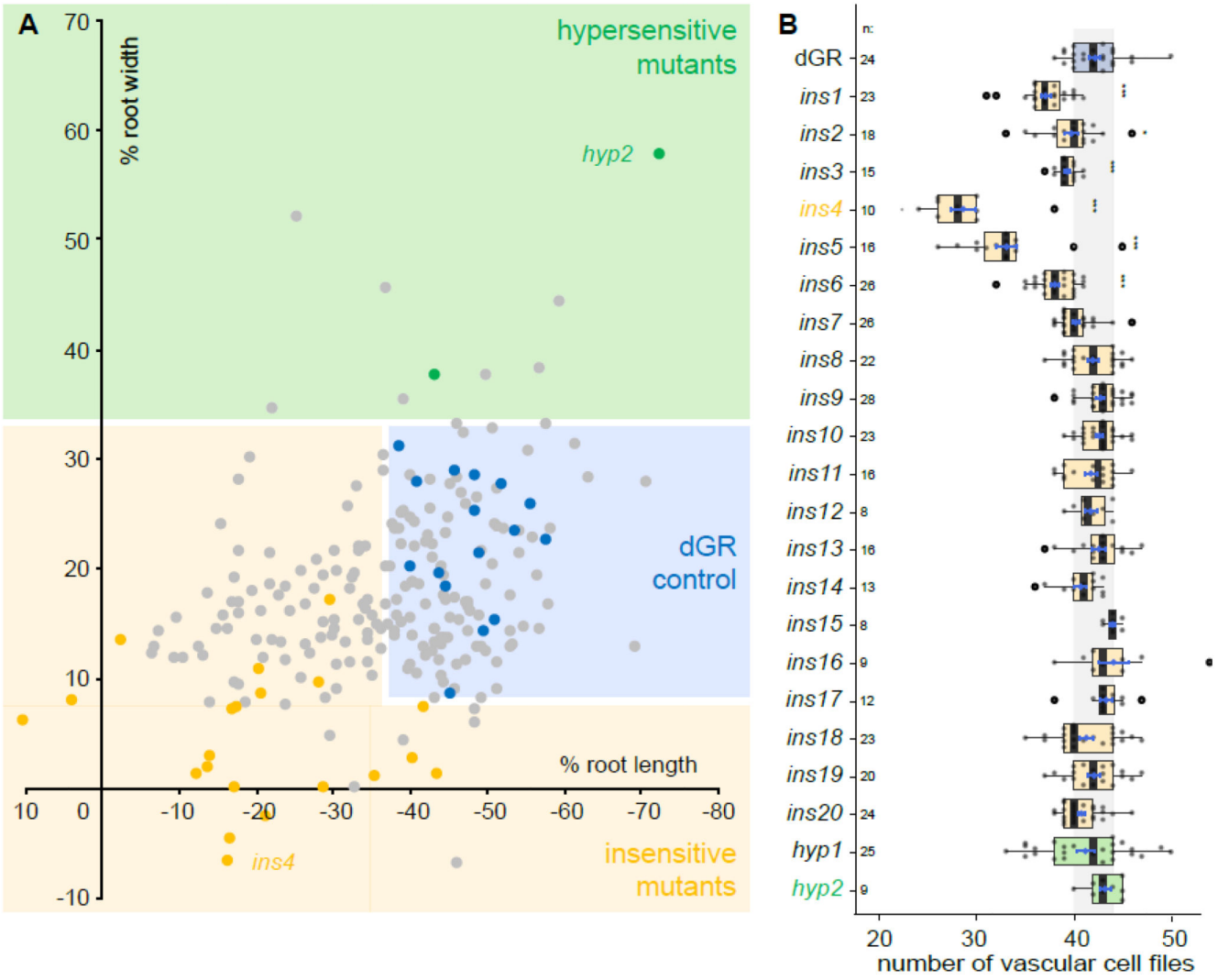

Figure 2. Overview of obtained EMS mutants.

(A) A total overview of all 260 primary selected EMS mutants and several parental dGR lines, plotted for their sensitivity of root length changes against the sensitivity of root width changes relative to mock treatment of the same genotype. Thus, the percentage represent mock vs DEX treatment of each mutant or parental dGR line. Data from the EMS screening was used. Dots in the blue box represent EMS mutants behaving similar to parental dGR control and dots in the yellow box represent mutants that behave insensitive to dGR response (significant longer and/or thinner roots) compared to the dGR parental line, while in the green box mutants behave hypersensitive to dGR induction. Yellow and green dots represent the 22 selected EMS mutants, the yellow dots represent the *ins* mutants and green dots the *hyp* mutants. Grey dots represent other EMS mutants selected from the primary screen and blue dots represent non-mutagenized parental dGR. Each data point was compared with a dGR parental control grown on the same plate. This internal control explains why some non-significant EMS mutant lines (grey dots) are further away from the parental dGR (blue dots) then some significant EMS mutant lines (yellow or green dots). For each data point

the average was used from 10 biological repeats. **(B)** Overview vascular cell files phenotype in candidate mutants. Counts of vascular cell files in the root meristem of 1-week-old dGR (blue), *ins* (yellow) and *hyp* (green) seedlings. All genotypes described contain the dGR constructs. Black lines indicate the median and boxes indicate data ranges. The mean and its precision are plotted as the blue rhombus with blue SE bars. The n is above the genotype labels indicates number of datapoints for each genotype. Pairwise comparisons with Dunnett method p-value adjustment, was performed to evaluate significant differences between a mutant's and dGR number of vascular cell files (**Table S1**). Significances asterisks: * = p-value < 0.05; ** = p-value < 0.01; *** = p-value < 0.001.

Europe PMC Funders Author Manuscripts

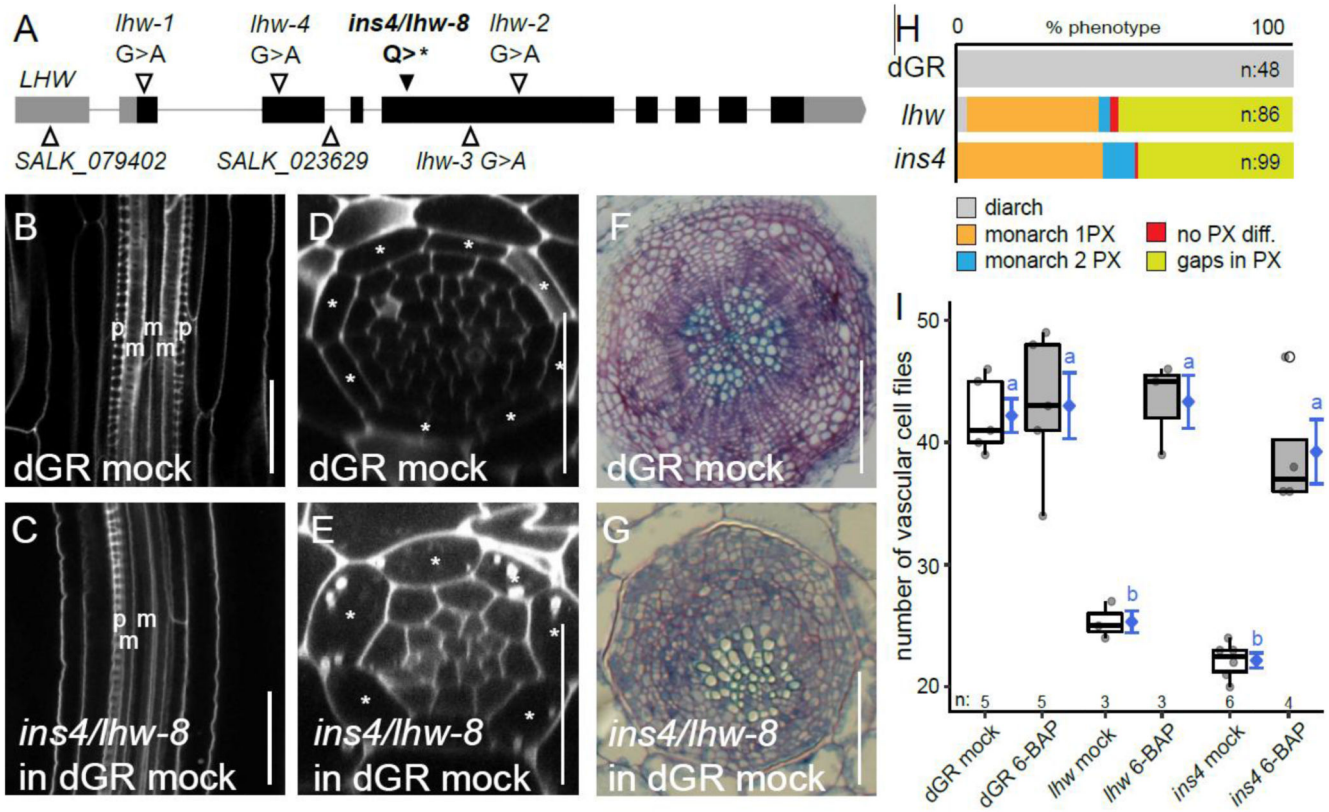

Figure 3. The insensitive mutant *ins4* is a novel *lhw* allele.

(**A**) Alleles of *lhw* mutants with *ins4*/*lhw-8* having a point mutation, resulting in a premature stop codon in exon (black bar) 4 of *LHW*. (**B-C**) Longitudinal view of the root vascular tissue shown for dGR (**B**) and *ins4*/*lhw-8* (dGR) (**C**). (**D-E**) Optical cross-section through the root meristem of dGR (**D**) and *ins4*/*lhw-8* (dGR) (**E**) show smaller vascular cylinder for *ins4*/*lhw-8* (dGR). (**F-G**) Secondary growth phenotype can be observed in sections of dGR (**F**) and *ins4/lhw-8* (dGR) (**G**) through the hypocotyl of 3-week-old seedlings. Scale bars in B-E are 25 μm and in F-G 100 μm. (**H**) The frequency of xylem differentiation (diff.) phenotype plotted for dGR, *lhw* and *ins4* (dGR). The asterisks mark the endodermis cells in D-E, ‘p’ an ‘m’ represent protoxylem and metaxylem cell files in B-C. (**I**) The number of vascular cell files of 1-week-old seedlings treated with cytokinin (6-BAP). Black lines indicate mean values and grey/white boxes indicate data ranges. n marks the number of datapoints for each sample. The mean and its precision are plotted as the blue rhombus with blue SE bars. Count data samples were compared pairwise based estimated means of a generalized linear model with log link function. Common blue lower-case letters (compact letter display) at these means indicate non-significantly different groups as determined by the pairwise comparisons (**Table S1**).

Europe PMC Funders Author Manuscripts

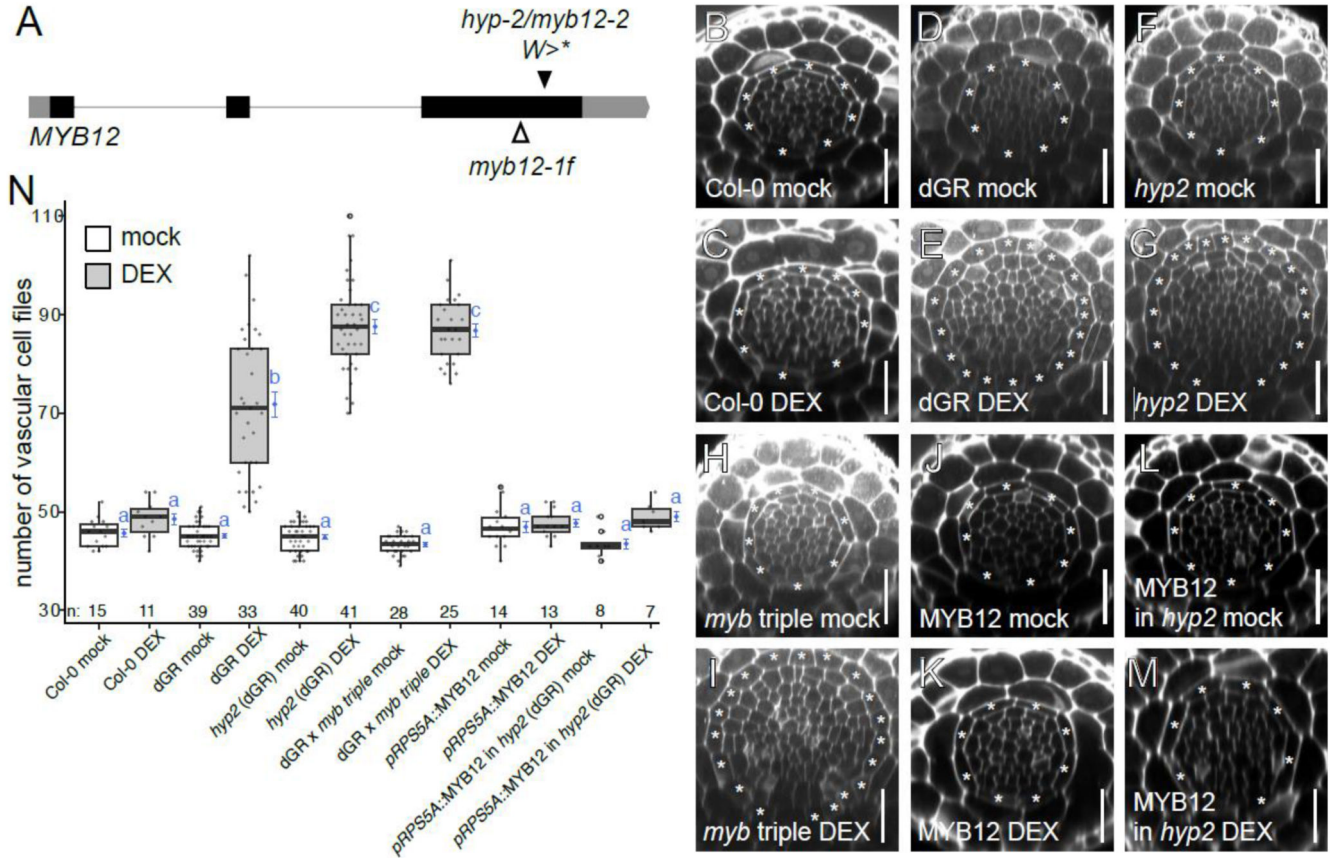

Figure 4. The *hyp2* is hypersensitive to dGR response and MYB12 acts as a repressor for TMO5/LHW activity.

(**A**) MYB12 gene marked with known *myb12-1f* transposon insertion site and hyp2/*myb12-2* point mutation site, which results in premature stop codon. (**B**-**M**) Representative root meristem cross-sections of Col-0 on mock (**B**), Col-0 on DEX (**C**), dGR on mock (**D**), dGR on DEX (**E**), *hyp2*/myb12-2 (dGR) on mock (**F**), *hyp2*/myb12-2 (dGR) on DEX (**G**), *myb11 myb12-1f myb111* triple mutant (referred to as *myb triple*) (dGR) on mock (**H**), myb triple (dGR) on DEX (**I**), p*RPS5A*::MYB12 on mock (**J**), p*RPS5A*::MYB12 on DEX (**K**), p*RPS5A*::MYB12 (in *myb12-2* (dGR)) line on mock (**L**) and on DEX (**M**). The asterisks mark the endodermis cells and counted vascular cell file number are within this cell type. Scale bars are 25 μm. (**N**) Boxplot plotting the vascular cell file number. Black lines indicates mean values and grey/white boxes indicate data ranges. n marks the number of datapoints for each sample. The mean and it precision are plotted as the blue rhombus with blue SE bars. Count data samples were compared pairwise based estimated means of a generalized linear model with log link function. No shared blue lower-case letters (compact letter display) at these means indicate significantly different groups as determined by the pairwise comparisons (**Table S1**).

Europe PMC Funders Author Manuscripts

Europe PMC Funders Author Manuscripts

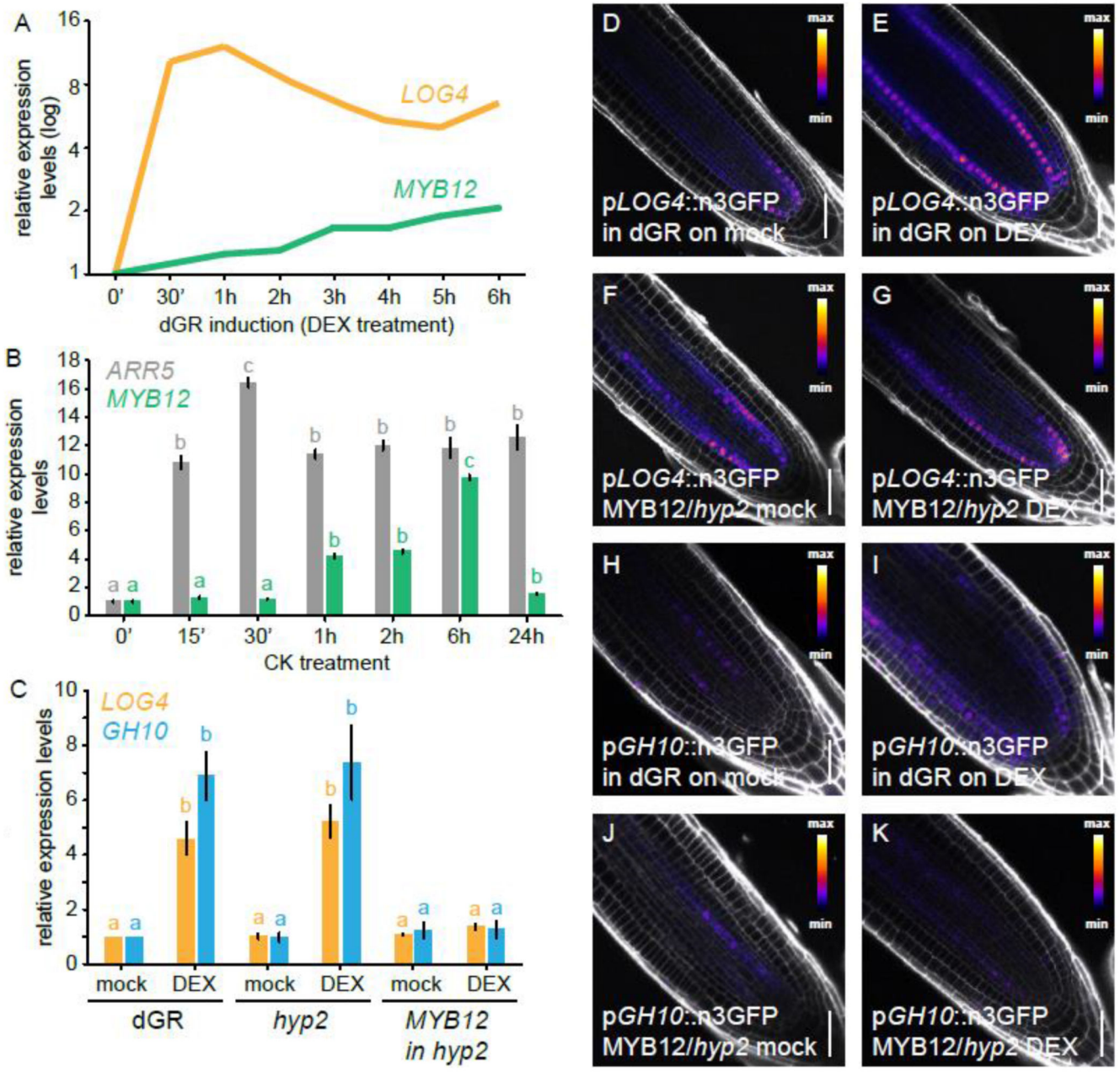

Figure 5. MYB12 acts downstream of TMO5/LHW-mediated CK production and represses TMO5/LHW targets.

(**A**) Relative expression levels *LOG4* and *MYB12* genes over different DEX treatment durations on dGR line derived from microarray data described in Smet et al 2019 (Smet *et al.*, 2019), with 0h DEX expression levels set to 1. (**B**) Relative expression levels of the CK-inducible A-type *ARR5* and *MYB12* in a time course experiment following cytokinin treatment. **(C)** Relative expression of LOG4 and GH10 in 5-days-old seedlings of dGR, hyp2/myb12-2 (dGR) and pRPS5A::MYB12 in hyp2/myb12-2 (dGR) where TMO5/LHW activity was induced for 2h on mock or DEX. Common lower-case letters in B, C indicate non-significantly different groups as determined by respectively one-way

and two-way ANOVA with post-hoc Tukey testing. Error bars are standard errors. (**D**-**G**) Expression of p*LOG4*::n3GFP in F1 5-days-old seedlings in dGR background (**D**-**E**) and p*RPS5A*::MYB12 in *hyp2/myb12-2* (dGR) (**F**-**G**) background after 24h on mock (**D**,**F**) or DEX (**E**,**G**). Expression of p*GH10*::n3GFP in F1 5-days-old seedlings in dGR background (**H**-**I**) and p*RPS5A*::MYB12 in *hyp2/myb12-2* (dGR) background (**J**-**K**) after 24h on mock (**H**,**J**) or DEX (**I**,**K**). Scale bars are 50 μm.

Europe PMC Funders Author Manuscripts

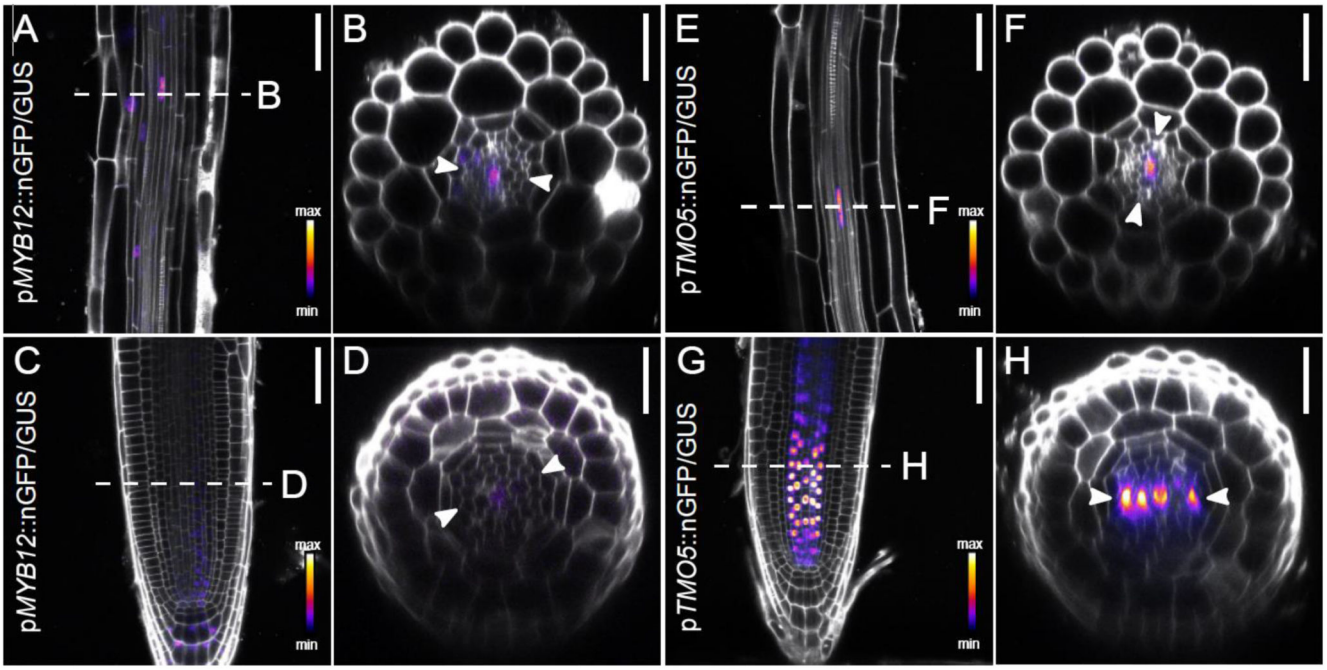

Figure 6. MYB12 and TMO5 have overlapping expression patterns in root tissues.
(**A-B**) Expression pattern of 1-week-old p*MYB12*::nGFP/GUS in root elongation zone and (**C-D**) root meristem. (**E-F**) Expression pattern of 1-week-old p*TMO5*::nGFP/GUS in root elongation zone and (**E-F**) and (**C-D**) root meristem. The dashed line marks location optical cross section was made. Arrowheads indicate xylem axis in optical cross sections. Scale bars are 50 μm (**A**,**C**,**E**,**G**) and 25 μm (**B**,**D**,**H**,**F**).

Europe PMC Funders Author Manuscripts

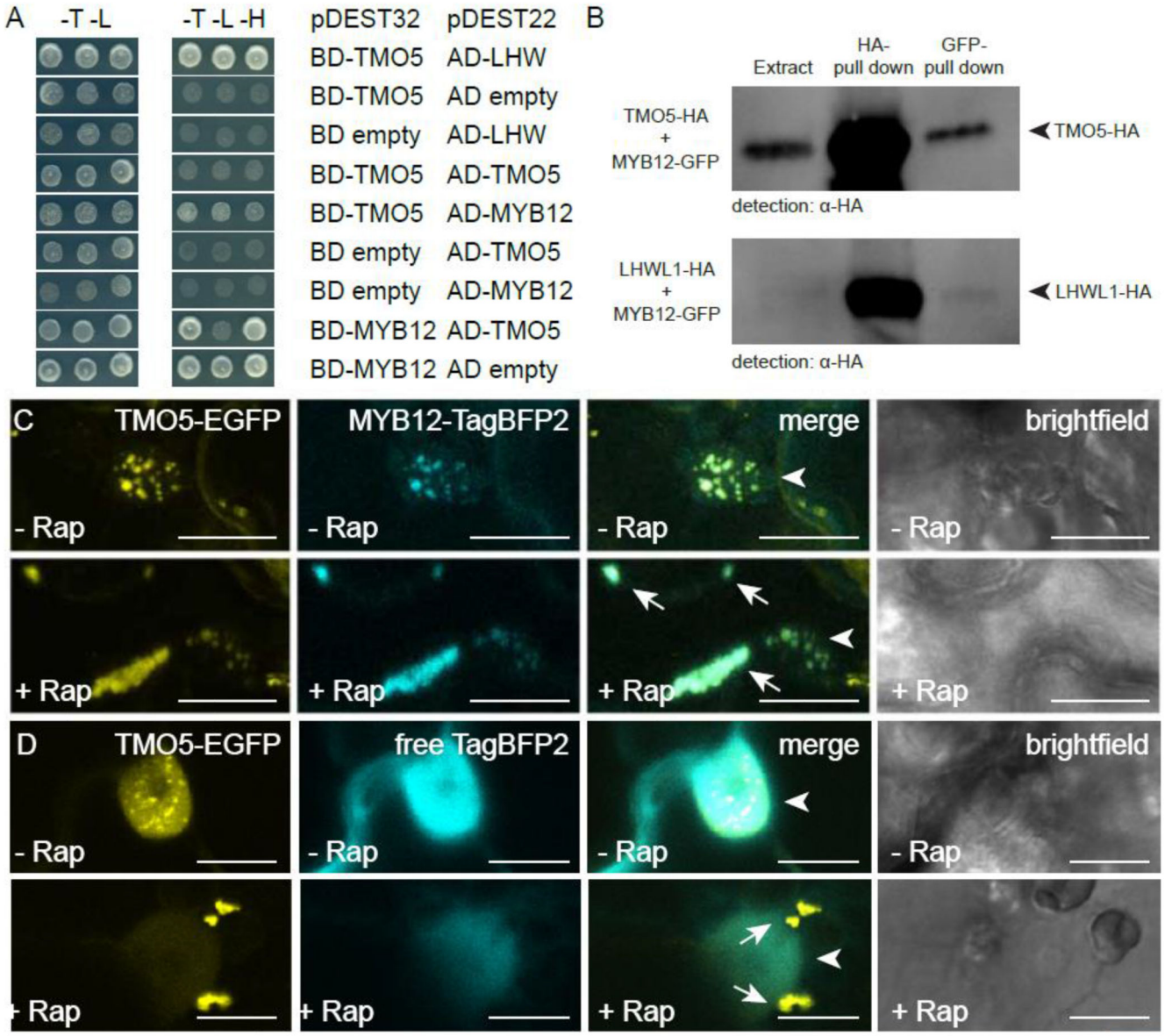

Figure 7. MYB12 binds to TMO5 in yeast and tobacco leaves.

(**A**) Yeast-two-hybrid assay with pDEST22 (prey) or pDEST32 (bait) constructs containing fusion proteins of the MYB12 and TMO5 coupled to respectively, the activator (AD) or binding domain (BD). The yeast colonies are representative colonies of 24 independent yeast transformants per prey and bait pair. The empty pDEST22 or empty pDEST32 plasmids were used to check for auto-activation. Transformed yeast grown on the selective -Trp/-Leu (-T -L) medium and interaction verifying - Trp/-Leu/-His (-T -L -H) medium. (**B**) co-immunoprecipitation of TMO5-HA and LHW-LIKE1-HA with MYB12-GFP (full blot is shown in Figure S13). (**C-D**) Knock-sideways with Mito-FRB, TMO5-EGFP-FKGP and MYB12-TagBFP2 (C) or free TagBFP2 (D) as control in absence or presence of rapamycin.

Arrows indicate the aggregated mitochondria and arrowheads indicate the nucleus. (n ≥10 for C and n ≥20 for D) Scale bars are 20 μm in C and 10 μm in D.

Europe PMC Funders Author Manuscripts